9. Forward-flight performance

2020

Prof. SangJoon Shin

Overview

- I. Basic performance eqn.
- II. Calculation of drag-lift ratios
- III. Profile drag-lift ratio charts
- IV. Climb performance calculations
- V. Range and endurance calculations
- VI. Experimental data and comparison with theory
- VII. Effects of airfoil characteristics on performance

Introduction

- "Exact" performance method … necessarily involves the use of tables and charts in order to facilitate the work.
  - ① "Energy" method … power expended at MR shaft must equal the sum of all the power losses expended by the rotor and fuselage
  - ② "Balance of force" method … the resultant force on the helicopter in steady flight = 0

    → ① must be accurate and available

Definition of reference axes

I. Basic performance eqn.

- Various sources of power expended by a helicopter in steady flight

1) Rotor
   a. Induced power loss
   b. Blade profile-drag loss
2) Parasite drag (fuselage, rotor hub, TR)
3) Power necessary to change PE of a helicopter of a given rate of speed in the climb or glide condition

$$HP_{total} = HP_0 + HP_i + HP_p + HP_c \quad (1)$$

Definition of reference axes

- Each individual power

  → energy dissipated per second by an equivalent drag force moving at the translation velocity

  P: total equivalent drag force (not power)

$$\left.\begin{aligned} D_0 V &= HP_0 \\ D_i V &= HP_i \\ D_p V &= HP_p \\ D_c V &= HP_c \\ PV &= HP_{total} \end{aligned}\right\} \qquad (2)$$

(2) → (1) $P = D_0 + D_i + D_p + D_c$ (3)

Definition of reference axes

- Non-dimensionalize by the rotor lift L

$$\frac{P}{L} = \left(\frac{D}{L}\right)_0 + \left(\frac{D}{L}\right)_i + \left(\frac{D}{L}\right)_p + \left(\frac{D}{L}\right)_c \qquad (4)$$

- Rotor drag-lift ratio

$$\left(\frac{D}{L}\right)_r = \left(\frac{D}{L}\right)_0 + \left(\frac{D}{L}\right)_i \qquad (5)$$

- $\frac{P}{L}$: total rotor-shaft power input and is analogous to the drag-lift ratio of an airplane

$$\frac{P}{L} = \frac{shaft\,power}{VL} = \frac{Q\Omega}{VL} \qquad (6)$$

Calculation of drag-lift ratios

II. Calculation of drag-lift ratios

① Induced drag-lift ratio

Chap. 8 Eq. (75) →

$$\left(\frac{D}{L}\right)_i = \frac{C_T}{2\mu\sqrt{\mu^2+\lambda^2}} \qquad (7)$$

- $L = T\ cos\alpha$, (7) →

$$\left(\frac{D}{L}\right)_i = \frac{C_T}{4}\left[\frac{\mu}{\cos^3\alpha\sqrt{\mu^2+\lambda^2}}\right] \qquad (8)$$

When $\mu > 0.1$, the bracketed expression in eqn. (8) may be considered equal to unity →

$$\left(\frac{D}{L}\right)_i \cong \frac{C_L}{4}$$

Calculation of drag-lift ratios

- Fixed airplane wing … uniform downwash distribution →

  Amount of air influenced by the rotor per second

  $= R \times V$(flight speed)

- Momentum considerations

$$L = \pi R^2 \rho V (2v) \tag{9}$$

$= \text{Eq. (3) in Chap. 8 when} \begin{cases} \alpha = 0 \\ contribution\ of\ v\ negligible \end{cases}$

$$\frac{D_i}{L} = \left(\frac{D}{L}\right)_i = \frac{v}{V} \tag{10}$$

$$(9), (10) \rightarrow \left(\frac{D}{L}\right)_i = \frac{L}{2\pi R^2 \rho V^2} = \frac{C_L}{4} \tag{11}$$

at all speeds except near hover or at large α

→ use (7) or (8)

Calculation of drag-lift ratios

② Parasite drag-lift ratio

- Parasite drag force of the fuselage, rotor hub, and all the non lifting components

$$D_p = C_{D_p} \frac{1}{2} \rho V^2 \pi \mathrm{R}^2 \qquad (12)$$

- Single parameter … equivalent flat-plate drag area

$$D_p = f \frac{1}{2} \rho V^2 \qquad (13)$$

- Dividing by lift

$$\left(\frac{D}{L}\right)_p = \frac{f \frac{1}{2} \rho V^2}{L} = \frac{1}{C_L} \frac{f}{\pi R^2} \qquad (14)$$

Calculation of drag-lift ratios

③ Climb drag-lift ratio

-

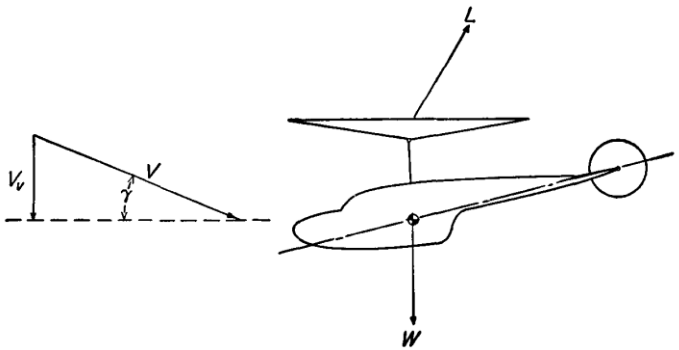

Fig. 9–1 Helicopter in climb.

… climb angle γ,

vertical rate of climb V_v

$$D_c V = W V_v,\ D_c = W\frac{V_v}{V} \qquad (15)$$

- $W = \frac{L}{\cos\gamma}, \frac{V_v}{V} = \sin\gamma$

$$(15) \rightarrow :\ \left(\frac{D}{L}\right)_c = \tan\gamma \qquad (16)$$

- For small angle of climb $\left(\frac{D}{L}\right)_c = \frac{V_v}{V}$ (17)
- Descending, $\left(\frac{D}{L}\right)_c$ (-)

Calculation of drag-lift ratios

④ Profile drag-lift ratio

- Profile drag-lift ratio … should involve items such as the blade pitch angle, rotor inflow (should first be known).

Chap. 8, Eq. (73) →

$$\mu \frac{2C_T}{\sigma a}\left(\frac{D}{L}\right)_0 = \frac{\delta_0}{a}\left(t_{,6,1}\right) + \frac{\delta_1}{a}\left[\left(t_{6,2}\right)\lambda + \left(t_{6,3}\right)\theta_0 + \left(t_{6,4}\right)\theta_1\right]$$

$$+\frac{\delta_2}{a}\left[\left(t_{6,5}\right)\lambda^2 + \left(t_{6,6}\right)\lambda\theta_0 + \left(t_{6,4}\right)\lambda\theta_1 \qquad (18)$$

$$+\left(t_{6,8}\right)\theta_0^2 + \left(t_{6,9}\right)\theta_0\theta_1 + \left(t_{6,10}\right)\theta_1^2\right]$$

$$c_{d_0} = \delta_0 + \delta_1\alpha_r + \delta_2\alpha_r^2 \qquad (19)$$

… known except λ and θ ← Eqs. (69), (71), Chap. 8

$$C_T = f(\lambda, \theta, \mu), C_Q = f(\lambda, \theta, \mu)$$

Calculation of drag-lift ratios

- However, C_Q needs to be assumed to obtain profile-drag contribution
  → trial and error process
  1) Assume C_Q, solve for λ, θ
  2) λ, θ in (1) → $\left(\frac{D}{L}\right)_0$ in Eq. (18)
  3) $\frac{P}{L}$ by Eq. (4) (9)
  4) $\frac{P}{L}$ → Q, C_Q by Eq. (6)
  5) Compare C_Q between assumed and by (4), repeat (1)~ (4)

- $\left(\frac{D}{L}\right)_0$ … by the use of charts

Profile drag-lift ratio charts

III. Profile drag-lift ratio charts

① Method of calculation … Figs. 9-2, 9-3: forward flight articulated rectangular untwisted blades

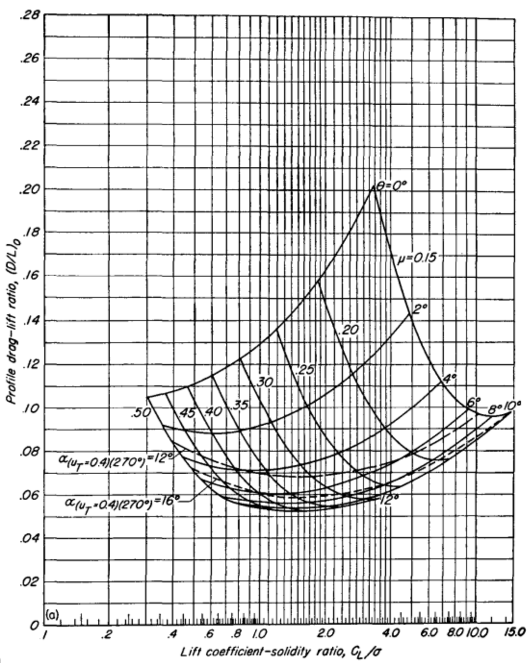

Fig. 9-2 Performance charts for computation of profile drag-lift ratios.
(a) $P/L = 0$

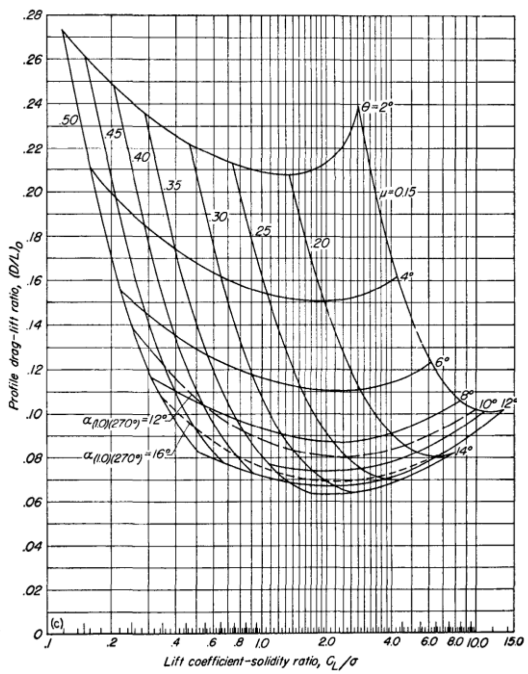

(c) $P/L = 0.2$

… lift vs. profile-drag characteristics in terms of θ, μ, σ for a particular value of $\frac{P}{L}$

Profile drag-lift ratio charts

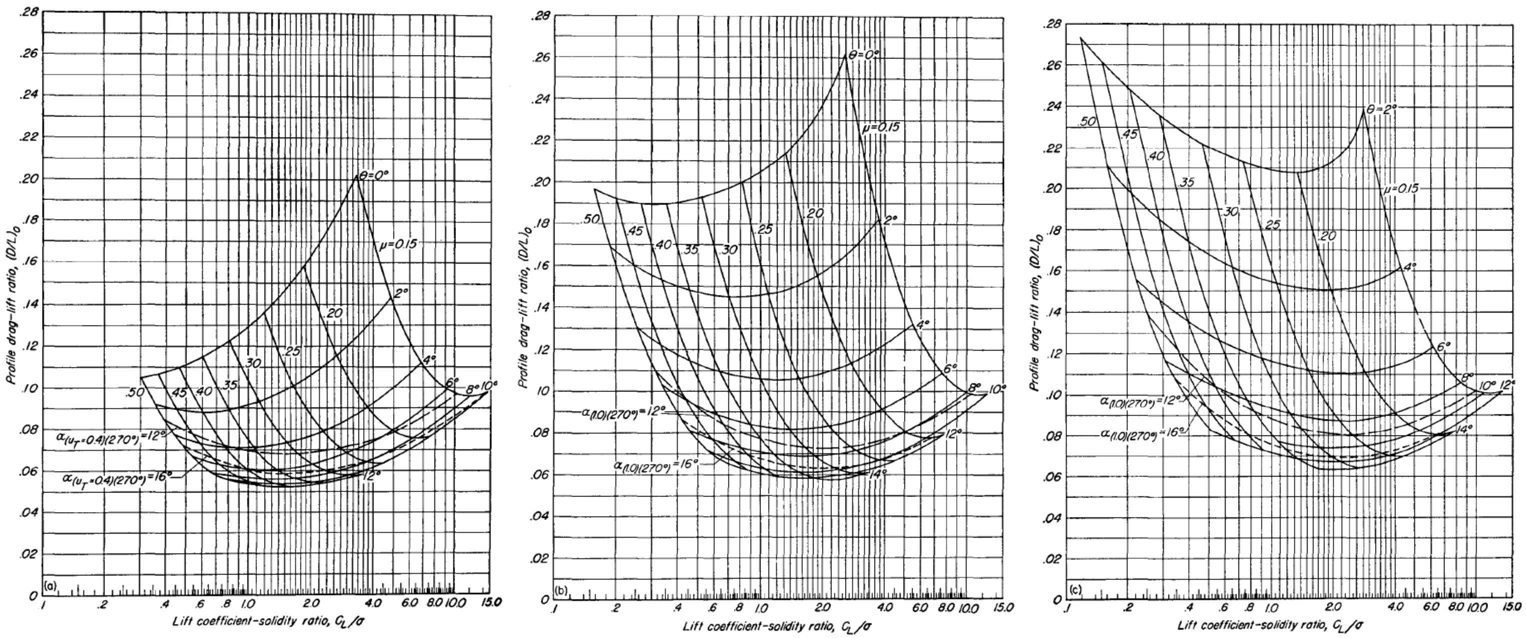

Fig. 9–2 Performance charts for computation of profile drag-lift ratios.
(a) P/L = 0

(b) P/L = 0.1

(c) P/L = 0.2

Profile drag-lift ratio charts

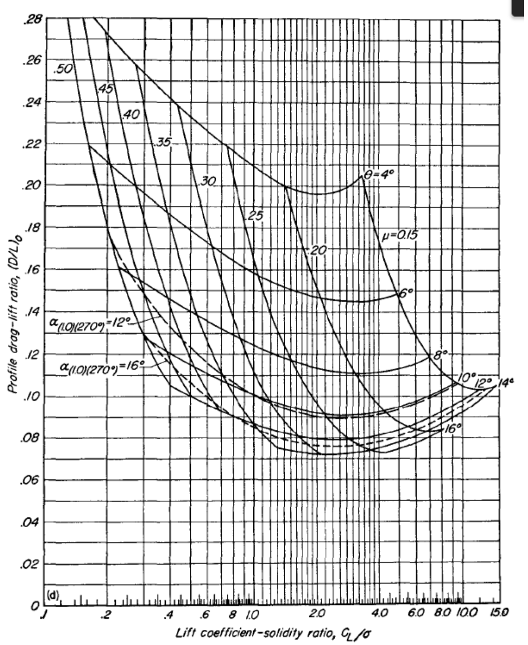

(d) $P/L = 0.3$

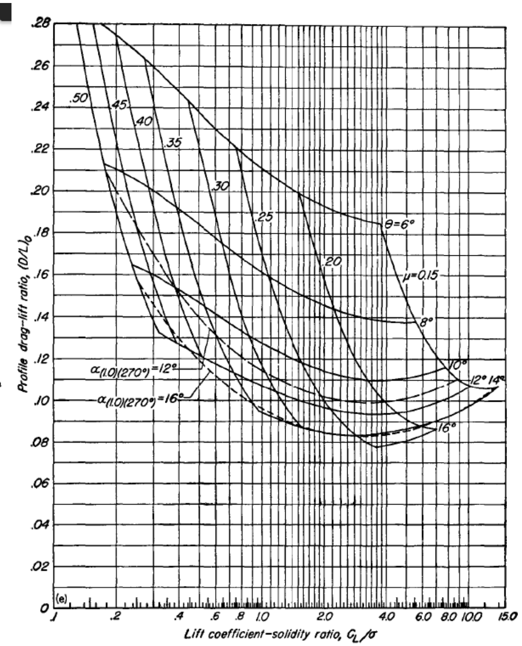

(e) $P/L = 0.4$

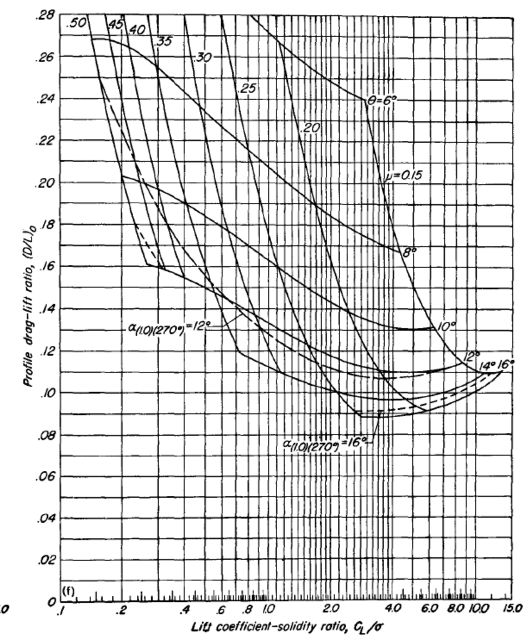

(f) $P/L = 0.5$

Profile drag-lift ratio charts

- Eq. (6), $L = T\cos\alpha$: $\rightarrow \frac{P}{L} = \frac{C_Q}{C_T \mu}$ (20)

$\cos\alpha = 1$,

$$W = C_L \frac{1}{2}\rho V^2 \pi R^2 = C_{\mathrm{T}} \pi R^2 \rho (\Omega R)^2$$

$$\frac{C_L}{\sigma} = \frac{2}{\mu^2}\frac{C_T}{\sigma} \quad (21)$$

for a fixed $\frac{D}{L}, \frac{2C_T}{\sigma a}, \frac{2C_Q}{\sigma}$ by Eqs. (20), (21)

$\lambda, \theta, \mu \rightarrow \left(\frac{L}{D}\right)_0$ by Eq. (18)

Profile drag-lift ratio charts

- Range of application
  - Same limitations arising from the theory development
  - $\gamma = 15$, but applicable to $\gamma = 0\sim 25$
  - Rectangular blade, but up to 3:1 taper ratio
  - Built-in twist = 0, but applicable to conventional twist

    Ex) $-8°$ built-in twist : 5% less profile drag than untwisted
  - Three-term drag curve $C_{d_0} = 0.0087 - 0.0216\alpha_r + 0.4\alpha_r^2$

    but applicable for rough or poorly built rotor blades by using "roughness" factor
  - AOA beyond stall → too optimistic prediction dotted lines of tip AOA $12°, 16°$ at the retreating blade

Profile drag-lift ratio charts

③ Sample calculation

level flight $V = 180\ fps$(106kts), $\mu = 0.2$ (tip speed = 900 fps)

D.L. = $2.5\ lb/ft^2$, $W = 3{,}140\ lb$, rectangular blade

built-in twist $=0$

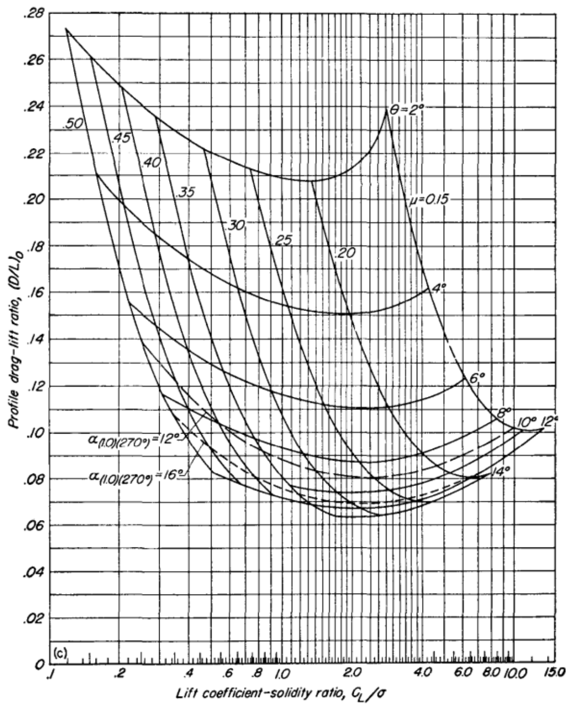

(c) $P/L = 0.2$

$$\left(\frac{D}{L}\right)_0 = 0.086$$

$$\left(\frac{D}{L}\right)_i = 0.082 \text{ (by } \frac{C_L}{4}\text{)}$$

$$\left(\frac{D}{L}\right)_p = 0.036$$

$$\left(\frac{D}{L}\right)_c = 0 \ (\because \text{ level flight})$$

$$\frac{P}{L} = 0.086 + 0.082 + 0.036 + 0 = 0.204$$

Profile drag-lift ratio charts

- 2nd approximation, $\left(\frac{D}{L}\right)_0$ interpolation

  between P/L=0.2 and P/L=0.3 → $\left(\frac{D}{L}\right)_0 = 0.086$, no further approximation

- Total rotor shaft power required

  $$\frac{0.204\times3140\times80}{550} = 93.2(hp)$$

- TR power absorption

  Control axis angle (+) … Autorotative condition, little or no power expended, MR supplies the power as a parasite drag

  Control axis angle (-) … Pulling TR in the air, MR expends certain power

Profile drag-lift ratio charts

$\mu = 0.2$, rectangular, non-twisted, $\sigma = 0.1$, $R_{TR} = 4ft$

Control axis angle = $0°$, MR distance = $25ft$

$$\Omega_{MR} \cong \frac{V}{\mu \mathrm{R}} = 20\, rad/sec,$$

$$\Omega_{TR} = 100\, rad/sec$$

Profile drag-lift ratio charts

- Thrust of TR

$$T_{TR} = \frac{hp_{MR} \times 550}{\Omega_{MR} \times 25} = 102.7\ lb, C_{T_{TR}} = 0.00536$$

- Inflow ratio … by Chap. 8, Eq. (8)

$$\alpha = \frac{\lambda}{\mu} + \frac{C_T}{2\mu^2} \quad (23)$$

$\alpha = 0, \lambda \rightarrow$: $\lambda = -\frac{C_T}{2\mu} = -0.0134$

$\rightarrow$ Eq. (69), Chap. 8 $\rightarrow$ $\theta = 4.47°$,

By Eq. (21) $\rightarrow \frac{C_L}{\sigma} = \frac{2C_T}{6\mu^2} = 2.68$

From chart, interpolation $\frac{P}{L} = 0.138$

$$hp_{TR} = \frac{P}{L} \times \frac{TV}{550} = 2.1\ (shp)$$

Profile drag-lift ratio charts

- Rater than P/L, sum of $\left(\frac{D}{L}\right)_0$ and $\left(\frac{D}{L}\right)_i$ contributes to the total power charged to torque counteraction

  at $\frac{P}{L} = 0.138, \left(\frac{D}{L}\right)_0 = 0.120$ from charts

$$\left(\frac{D}{L}\right)_i = \frac{C_L}{\sigma}\frac{\sigma}{4} = 0.067 \qquad (23)$$

  total $\left(\frac{D}{L}\right)_{TR} = 0.187 \; \rightarrow 2.8\ (hp)$

  $2.8 - 2.1 = 0.7\ (hp)$ should be supplied by *MR*

∴ revised *MR* rotor-shaft power = $93.2 + 0.7 = 93.9\ (hp)$

Profile drag-lift ratio charts

④ Effect of operating condition on profile drag

- Conditions of operation at which the rotor will perform most

  efficiently … $\begin{cases} induced\ losses\ \ldots fixed\ @particular\ speed \\ parasite \end{cases}$

  rotor profile drag loss … significant part of the total rotor losses,

  dependent on variables under designer's control

  (ex: blade pitch angle, rotor thrust/lift coeff., solidity)

- Minimum profile drag-lift ratio … any μ at the highest θ or

  at the highest rotor mean lift coeff. $(\frac{C_L}{\sigma})$

  ← high allowable section AOA at the retreating side or by operating as close to the stall limit lines as possible

- Chart → optimum μ for conventional design $\cong 0.25$

Climb performance calculations

IV. Climb performance calculations

- 2 alternate problems

① Rate of climb at a given V for given available power

② Power required to climb at a given rate of climb and V

- Procedure for Problem ①

1) P/L from the available power and gross weight (assume $W = L$)

2) $\frac{C_L}{\sigma}, \left(\frac{D}{L}\right)_i, \left(\frac{D}{L}\right)_P$ from the given W, V, h and rotor dimensions

3) $\frac{P}{L}, \frac{C_L}{\sigma}, \mu \rightarrow \left(\frac{D}{L}\right)_0$ from the charts

4) $\left(\frac{D}{L}\right)_c$ by Eq. (4)

Climb performance calculations

5) Rate of climb by Eq. (17)

- For large angle of climb γ, replace $L = W$ by $\mathrm{L} = W\cos\gamma$

  for power-off condition, omit Step (1). $\frac{P}{L} = 0$

- Sample helicopter, available $140\ hp$

1) $\frac{P}{L} = 0.306$

2) $\frac{C_L}{\sigma} = 4.7, \left(\frac{D}{L}\right)_i = 0.082, \left(\frac{D}{L}\right)_p = 0.036$

Climb performance calculations

3)

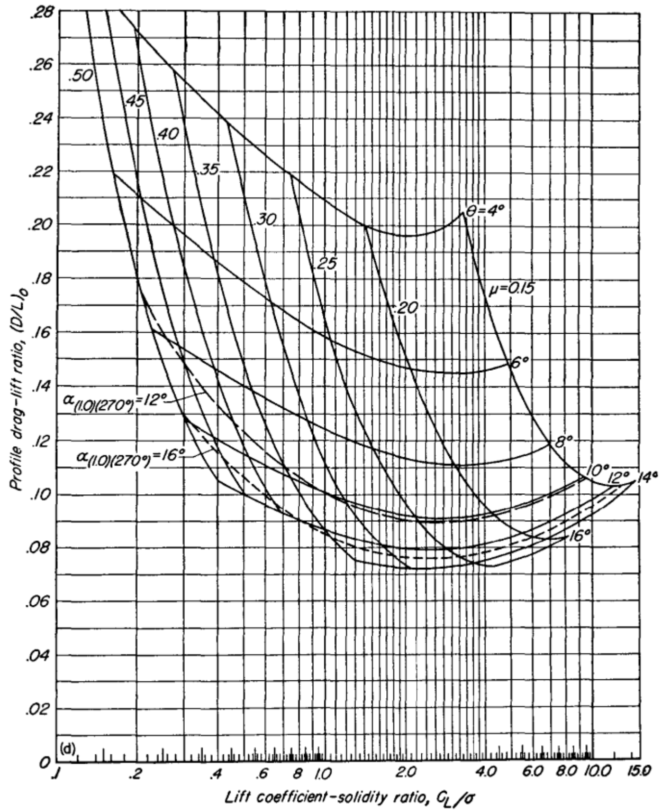

(d) $P/L = 0.3$

$$\rightarrow \left(\frac{D}{L}\right)_0 = 0.089$$

Climb performance calculations

4) $\left(\frac{D}{L}\right)_0 = 0.306 - 0.089 - 0.082 - 0.036 = 0.099$

5) $V_v = 0.099 \times 80fps = 475ft/min$

- Rate of climb vs. V for a typical helicopter

→

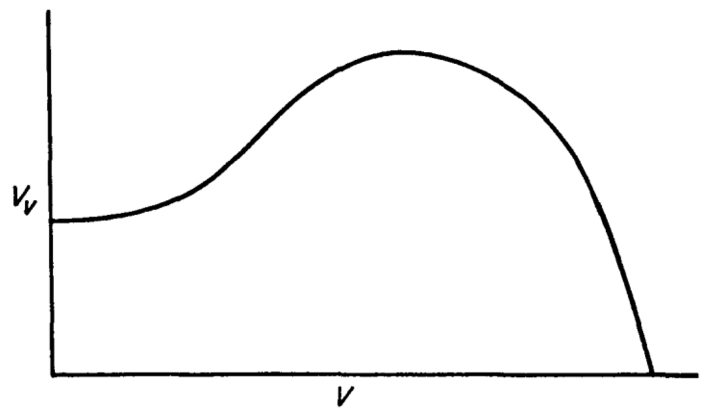

Fig. 9–4 Rate-of-climb curve for typical helicopter.

- For Problem ②, known value of $\left(\frac{D}{L}\right)_c$ is inserted before P/L is calculated.

Range and endurance calculations

V. Range and endurance calculations

- 2 alternate problems

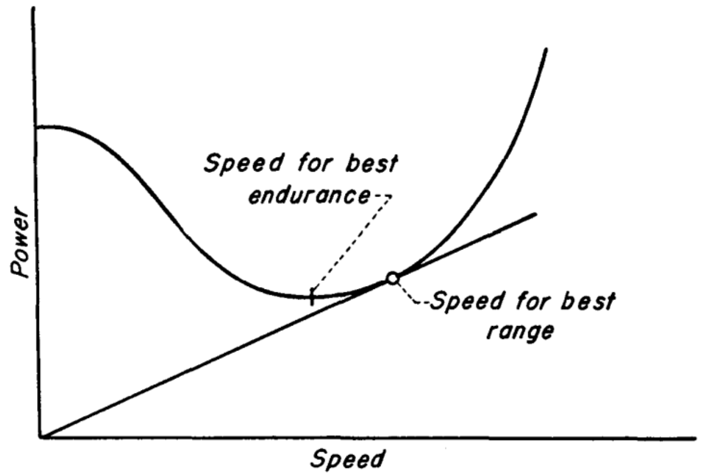

Fig. 9–5 Method of obtaining speed for best endurance and range.

… speed for best range: at the point at which the power required curve is tangent to a line drawn through the origin

At this point, the ratio of speed to power (of distance to fuel) is the greatest

- Best endurance … at the speed for minimum power

VI. Experimental data and comparison with theory

- Absence of good experimental data for forward flight

→ NACA, accurate flight and full-scale wind tunnel test data

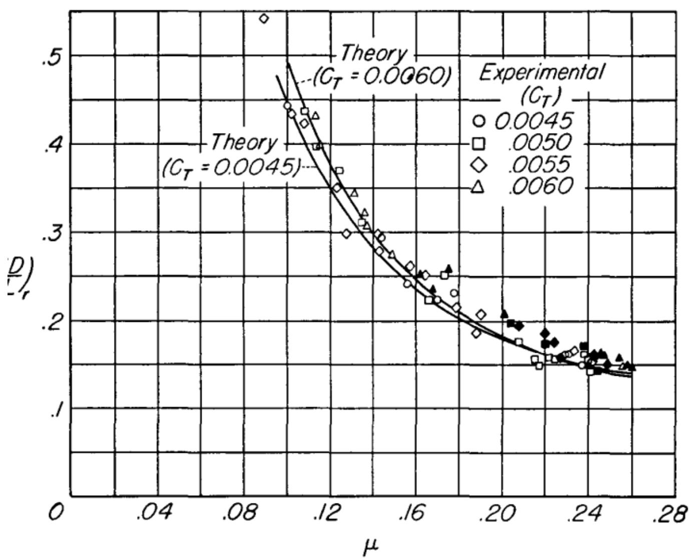

Fig. 9–6 Theory-data comparison for fabric-covered rotor in power-on flight.

… comparison of { the measured rotor performance / calculated }

- $\left(\frac{D}{L}\right)_r$ vs. μ, C_T
- AoA at the tip of the retreating blade $> 12°$

→ stall present

→ good agreement for the unstalled rotor

Experimental data and comparison with theory

- Different drag characteristics → rough, deformable, fabric-cover blades

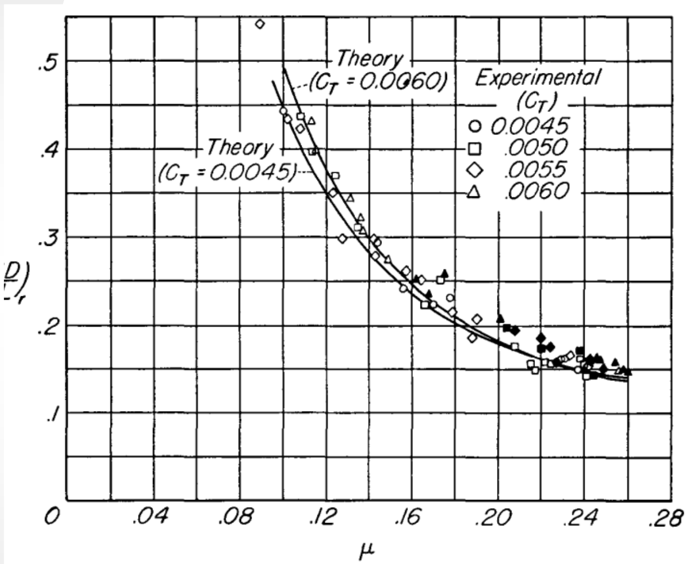

Fig. 9–6 Theory-data comparison for fabric-covered rotor in power-on flight.

… increased profile drag-lift ratio by 28%

- Equivalent to increasing the basic airfoil section drag by 50%

→ rotor-shaft power vs. V

gross weight = $2{,}560 lb$

$f = 15 ft^2$

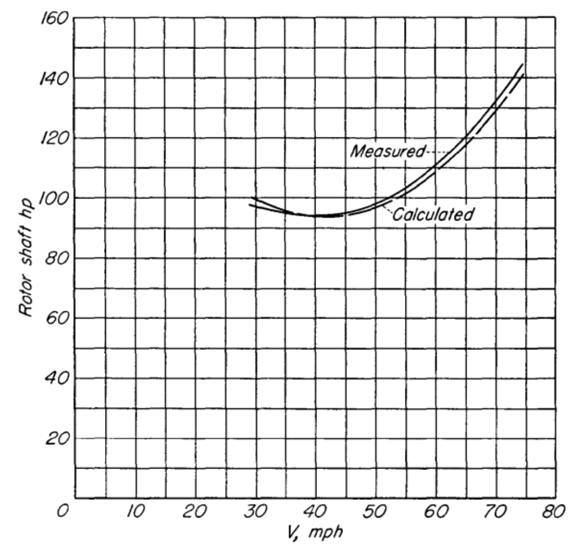

Fig. 9–7 Comparison of measured and calculated power required in power-on flight (from Appendix IIB, reference 20).

Experimental data and comparison with theory

•

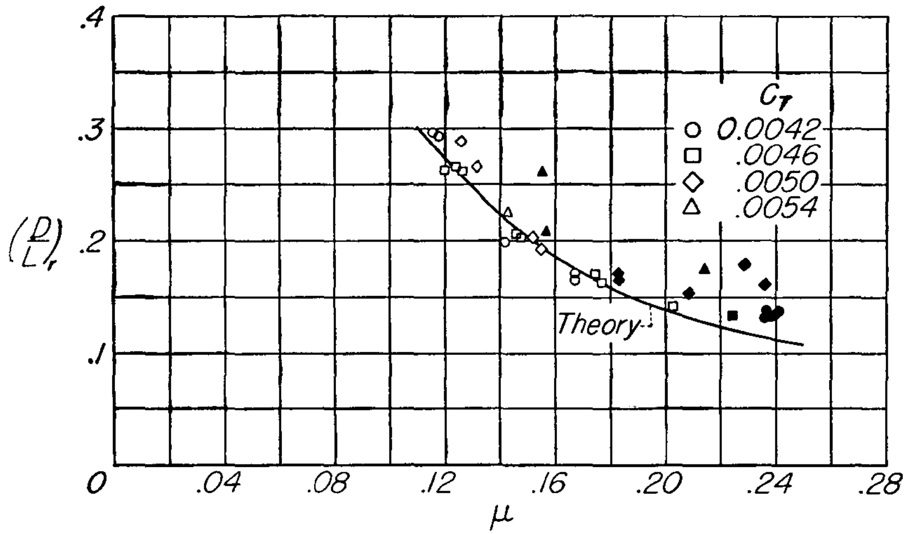

Fig. 9–8 Theory-data comparison for plywood-covered rotor in power-on flight.

… relatively smooth plywood-covered -8° twist

→ good agreement for the unstalled locations

Experimental data and comparison with theory

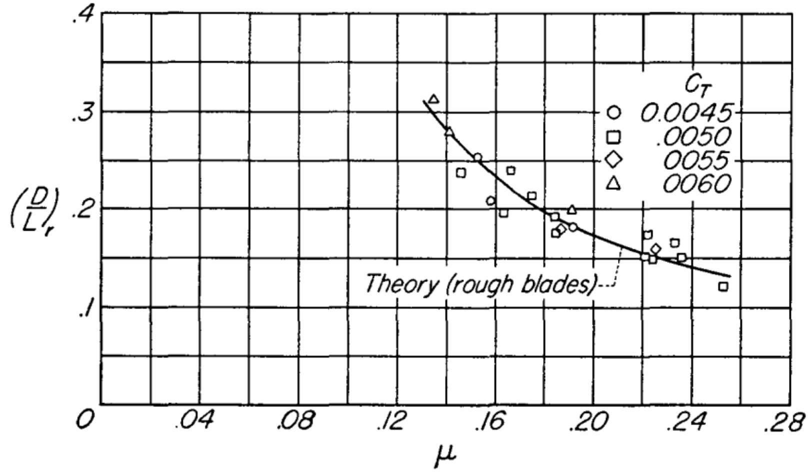

Fig. 9–9 Theory-data comparison for fabric-covered rotor in autorotation.

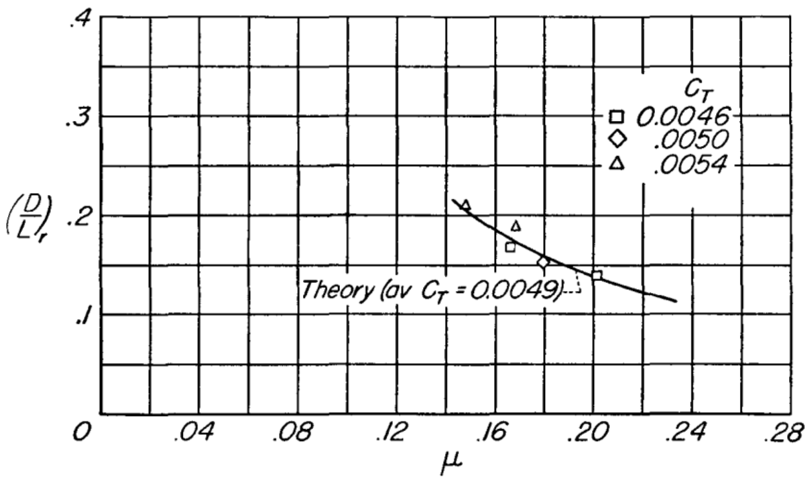

Fig. 9–10 Theory-data comparison for plywood-covered rotor in autorotation.

… Autorotative flight, $\frac{P}{L} = 0$

→ good fairing

∴ the present rotor theory may be used with confidence for the steady-flight characteristics

Static, 2-D airfoil characteristics can be applied to dynamic conditions.

VII. Effects of airfoil characteristics on performance

- Can be considered as occurring in 2 ways

① Variations in the profile-drag characteristics of the same airfoil

(different amount of blade production tolerance determination of the blade surface with age and use)

② Different blade properties

- Poorly built, fabric-covered blade with insufficient ribs

  … require 10% more power in hover, level flight in the minimum autorotative rate of descent

Effects of airfoil characteristics on performance

- Airfoil sections especially designed for rotors

  … high stall angle, high critical Mach number

  ① zero pitching moment

  ② Low drag throughout the range of low and moderate lifts

  ③ Moderate drag at high lifts

- Most NACA low-drag airfoils for wings and control surfaces

  → too high pitching-moment coeff.

  ↪ undesirable periodic stick forces, vibrations

  undesirable control-position gradients

  undesirable periodic blade twist

Effects of airfoil characteristics on performance

- Low-drag symmetric airfoil … not applicable low drag "bucket" (half of the limited range of lift coeff. where drag reductions are achieved is below zero lift) ← faster moving portions are at (+) lift coeff.

- Special airfoils by NACA … with NACA 23012

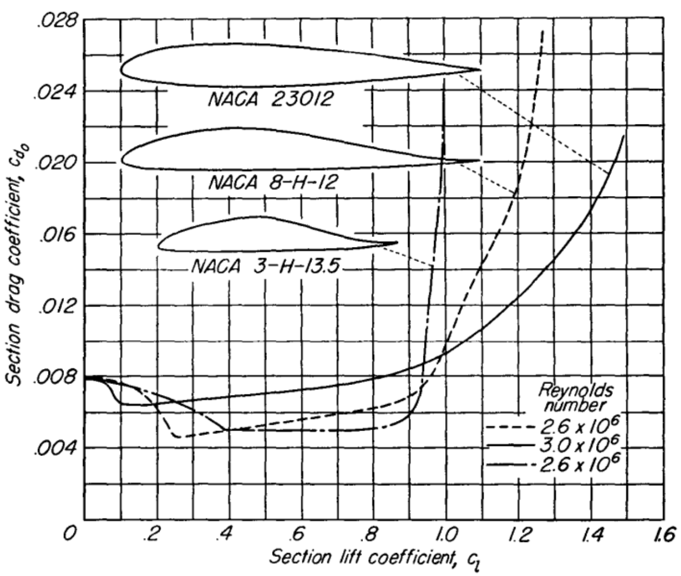

Fig. 9–11 Aerodynamic characteristics of conventional and helicopter airfoil sections.

8-H-12 section … lower drag over the lower range of lift coeff.,

3-H-135 section … but earlier and violent drag rise at higher angles

Effects of airfoil characteristics on performance

- 8-H-12 … superior to NACA 23012, but not sufficient information since blade section AoA varies from low to high
- Increment in drag coeff. has a smaller effect on the power absorbed at low velocity retreating side than at the high velocity advancing side
- 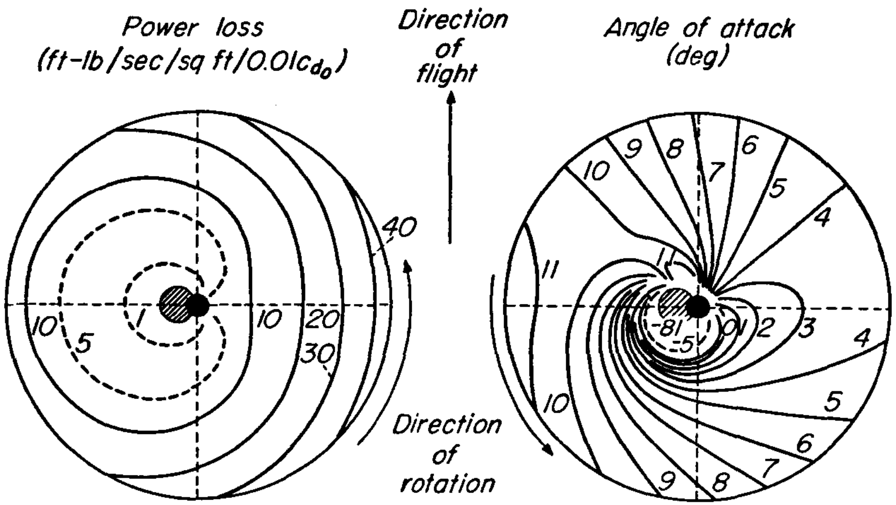

Fig. 9–12 Power loss and angle-of-attack contours: (V = 55 miles per hour; μ = 0.2; W/S = 2.5 pounds per square foot).

… AoA distribution, power loss distribution per unit value of profile-drag coeff. in cruise

Effects of airfoil characteristics on performance

•

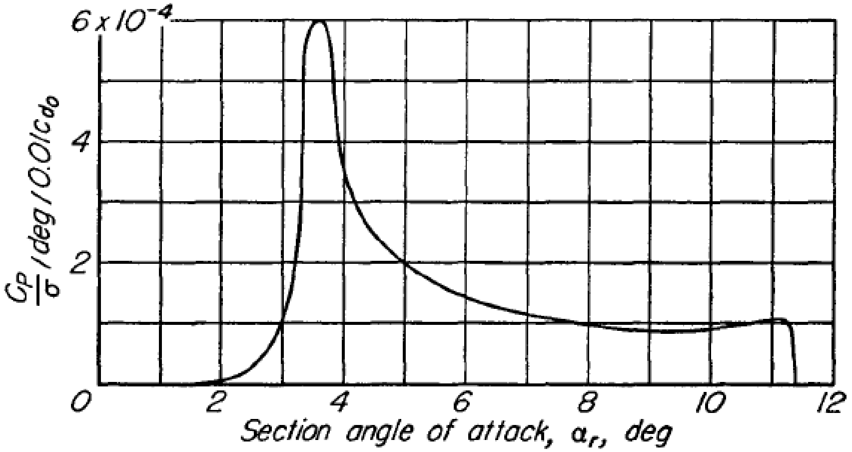

Fig. 9–13 Weighting curve for rotor of Fig. 9–12.

… "Weighting curve"

Power consumed in overcoming the profile drag by all the blade elements operating at a particular AoA for unit value of C_{d_0}

→ total profile drag power absorbed =

ordinate of the weighting curve × ordinate of C_{d_0} against AoA

Effects of airfoil characteristics on performance

•

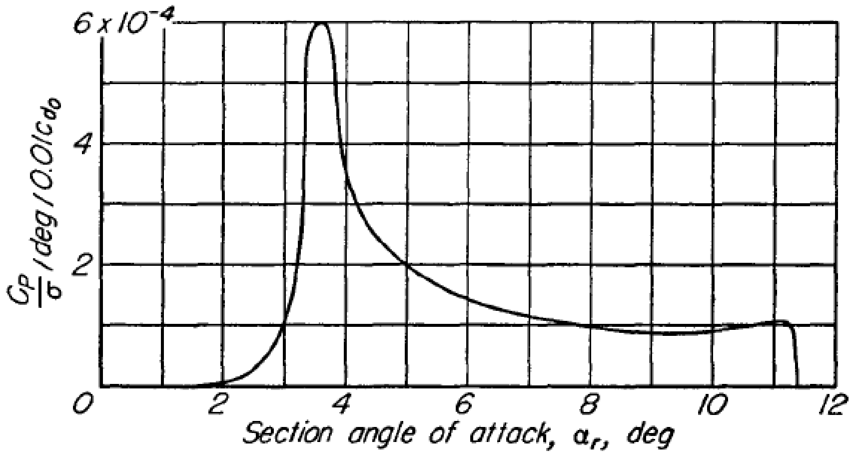

Fig. 9–13 Weighting curve for rotor of Fig. 9–12.

… great losses, occur at low AoA range, but significant losses also exist up to 12°

→ NACA 3-H-125 would not be appropriate

Effects of airfoil characteristics on performance

- Effect of drag-loss and μ from the weighting curve

→

TABLE 9—1

COMPARISON OF ROTOR-BLADE PROFILE-DRAG LOSS OF THE NACA 3-*H*-13.5, 8-*H*-12, AND 23012 AIRFOIL SECTIONS FOR VARIOUS FLIGHT CONDITIONS OF A SAMPLE HELICOPTER (FROM REFERENCES I-12 AND IV-4 OF APPENDIX IIA)
(R = 20 ft, ΩR = 400 fps, σ = 0.07, f = 15)

	Operating Conditions		Rotor-Blade Profile-Drag Loss, *HP*			Remarks
			NACA 3-*H*-13.5 Smooth	NACA 8-*H*-12 Smooth	NACA 23012 Smooth	
1	W/S = 1.55	μ = 0	16.0	14.4	20.1	Effect of loading (hovering flight)
2	3.33	0	14.5	18.5	24.1	
3	5.42	0	204.6	56.8	42.6	
4	μ = 0	W/S = 2.5	14.2	16.3	21.7	Effect of tip-speed ratio
5	0.2	2.5	23.2	21.2	25.7	
6	0.3	2.5	54.5	36.7	31.0	
7	W/S = 1.9	μ = 0.2	18.2	17.5	23.5	Effect of loading (forward flight)
5	2.5	0.2	23.2	21.2	25.7	
8	3.1	0.2	54.3	28.6	29.2	

- For the low loading, but high μ… 2 H profiles are 30% more efficient than 23012

- For the high loading and high μ… 3-H-13.5 is the worst due to early stall characteristics, 8-H-12 and 23012 similar power losses

∴ 8-H-12 superior to conventional sections